



# Identification of potent orally active factor Xa inhibitors based on conjugation strategy and application of predictable fragment recommender system



Tsukasa Ishihara<sup>a,\*</sup>, Yuji Koga<sup>a</sup>, Yoshiyuki Iwatsuki<sup>b</sup>, Fukushi Hirayama<sup>a</sup>

<sup>a</sup> Drug Discovery Research, Astellas Pharma Inc., 21, Miyukigaoka, Tsukuba-shi, Ibaraki 305-8585, Japan

<sup>b</sup> Pharmacovigilance, Astellas Pharma Inc., 2-5-1, Nihonbashi-Honcho, Chuo-ku, Tokyo 103-8411, Japan

## ARTICLE INFO

### Article history:

Received 16 October 2014

Revised 28 November 2014

Accepted 28 November 2014

Available online 5 December 2014

### Keywords:

Factor Xa

Conjugation

Recommender system

Collaborative filtering

## ABSTRACT

Anticoagulant agents have emerged as a promising class of therapeutic drugs for the treatment and prevention of arterial and venous thrombosis. We investigated a series of novel orally active factor Xa inhibitors designed using our previously reported conjugation strategy to boost oral anticoagulant effect. Structural optimization of anthranilamide derivative **3** as a lead compound with installation of phenolic hydroxyl group and extensive exploration of the P1 binding element led to the identification of 5-chloro-N-(5-chloro-2-pyridyl)-3-hydroxy-2-[(4-(4-methyl-1,4-diazepan-1-yl)benzoyl)amino]benzamide (**33**, AS1468240) as a potent factor Xa inhibitor with significant oral anticoagulant activity. We also reported a newly developed Free-Wilson-like fragment recommender system based on the integration of R-group decomposition with collaborative filtering for the structural optimization process.

© 2014 Elsevier Ltd. All rights reserved.

## 1. Introduction

In the industrialized world, thromboembolic disorders, such as ischemic stroke, deep venous thrombosis, myocardial infarction, unstable angina, and pulmonary embolism, are leading causes of morbidity and mortality. As thromboembolic disorders are triggered by excessive stimulation of the blood coagulation cascade, anticoagulants are used in the treatment and prevention of these diseases. The oral anticoagulant warfarin blocks biosynthesis of vitamin K-dependent coagulation factors and is prescribed for a growing number of indications. However, this drug takes several days to reach therapeutic blood concentration and has a narrow therapeutic index due to its indirect mechanism.<sup>1–4</sup> Therefore, significant medical needs have emerged for orally active direct anticoagulants with greater efficacy in treating and preventing blood clotting.

Numerous studies have been conducted to identify inhibitors of enzymes involved in the blood coagulation cascade. Thrombin was the initial target, followed by factor Xa (fXa). FXa acts at the juncture between the intrinsic and extrinsic pathways of the coagulation cascade and catalyzes the conversion of prothrombin to thrombin. Given that this enzyme is upstream from thrombin in the amplification of the coagulation cascade, inhibitors of fXa could

be more effective in attenuating the coagulation cascade than inhibitors of thrombin itself. Extensive preclinical data has shown that inhibition of fXa is effective in both venous and arterial thrombosis.<sup>5–7</sup> In addition, inhibition of fXa could be less likely to increase abnormal bleeding than direct inhibition of thrombin, because specific fXa inhibitors do not affect platelet activation and aggregation directly.<sup>8,9</sup> FXa has therefore emerged as an attractive target for new therapeutic agents with the potential to treat and prevent arterial and venous thrombosis.

A number of small molecule fXa inhibitors have been reported to date,<sup>10</sup> and their chemical structures are classified as amidine derivatives exemplified by the pioneer fXa inhibitor DX-9065a,<sup>11</sup> or nonamidine derivatives exemplified by rivaroxaban,<sup>12</sup> apixaban,<sup>13</sup> and edoxaban.<sup>14</sup> The benzamidine substituent of amidine derivatives forms a bidentate salt bridge interaction with the carboxylic acid of Asp189 in the S1 site of the enzyme. The high hydrophilicity of the amidine group increases the overall hydrophilicity of the molecule, which enables the enzymatic binding affinity to effectively translate into potent anticoagulant and antithrombotic activity.<sup>15,16</sup> However, the highly hydrophilic and basic profile of the amidine group also reduces membrane permeability and oral bioavailability of the inhibitor. In contrast, non-amidine inhibitors possess a less basic surrogate for the amidine group, such as an amine or aminomethyl that interacts with Asp189 or a small lipophilic substituent such as a methoxy or chloro group that occupies the small hydrophobic pocket formed by the residues

\* Corresponding author. Tel.: +81 29 863 6713; fax: +81 29 854 1519.

E-mail address: [tsukasa.ishihara@astellas.com](mailto:tsukasa.ishihara@astellas.com) (T. Ishihara).

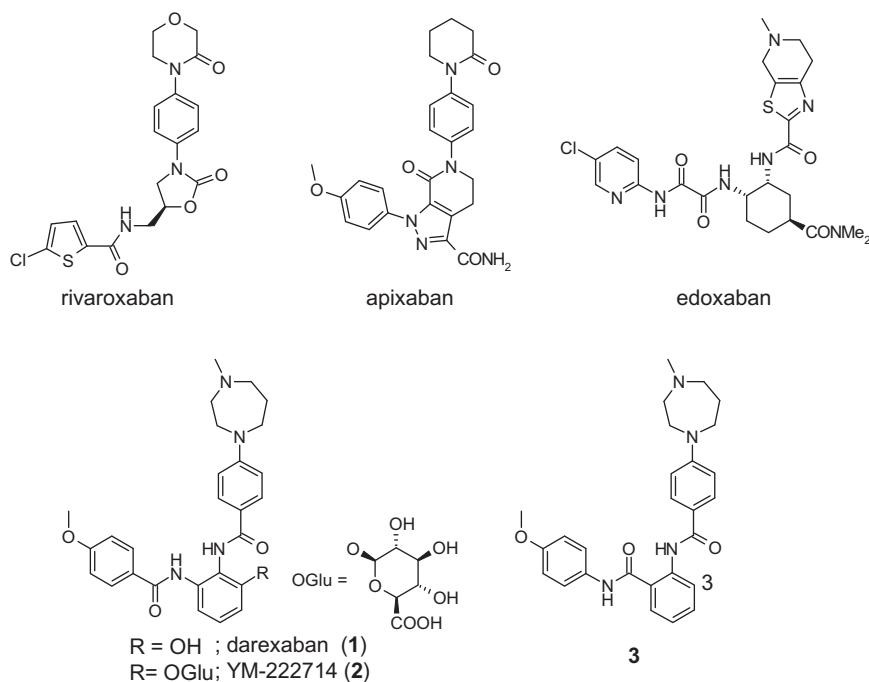
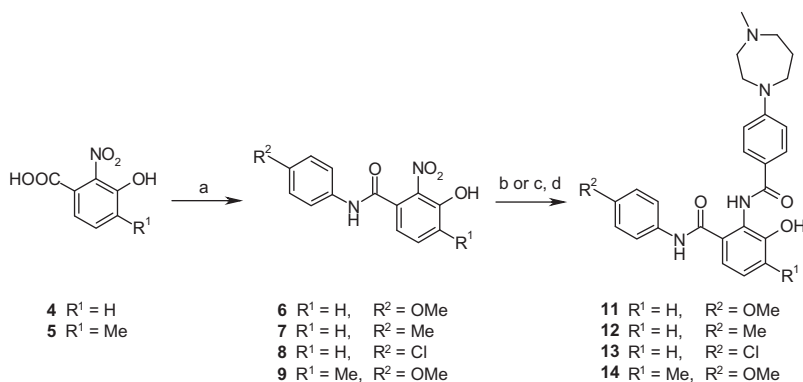


**Figure 1.** Structures of non-amidine type fXa inhibitors.



**Scheme 1.** (a) ArNH<sub>2</sub>, 1-hydroxybenzotriazole, 1-(3-dimethylaminopropyl)-3-ethylcarbodiimide hydrochloride, *N,N*-dimethylformamide (DMF); (b) H<sub>2</sub> (1 kgf/cm<sup>2</sup>), 10% Pd-C, ethanol; (c) Fe, NH<sub>4</sub>Cl, methanol, H<sub>2</sub>O, reflux; (d) Ar'COCl, pyridine.

of Ala190, Val213, and Tyr228 in the S1 site of the enzyme. Absence of a highly hydrophilic and basic amidine group often increases oral bioavailability of the inhibitor.<sup>10</sup>

We discovered two clinical candidates—YM466<sup>17</sup> and darexaban (**1**, Fig. 1).<sup>18</sup> In addition, we proposed a conjugation strategy to identify orally active inhibitors for enzymes in the coagulation cascade.<sup>19</sup> Our new methodology is based on nonamidine-based inhibitors that potentially have an improved oral absorption profile compared to amidine-based inhibitors. The key concept is an installation of a phenolic hydroxyl group, which works as a trigger moiety for glucuronide conjugation, into inhibitors. Biotransformation to glucuronide conjugates lowers lipophilicity of the inhibitors, demonstrating potent *in vivo* anticoagulant activity after administration.

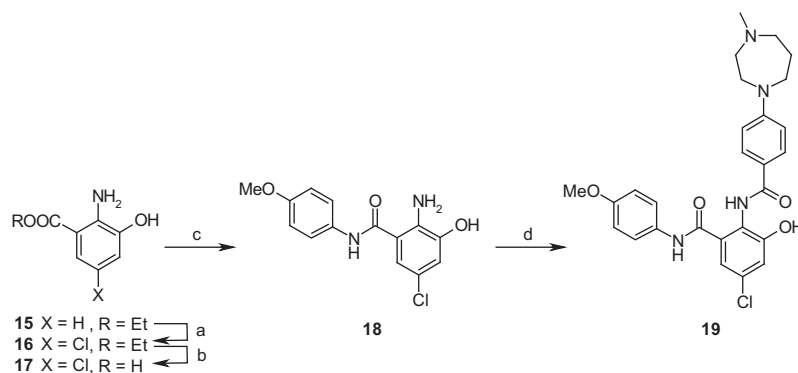
We also furnished up traditional Free-Wilson analysis<sup>20,21</sup> and framed a novel interpretable and predictable compound design workflow to recommend promising fragments in the structural optimization process. This methodology is based on a combination of R-group decomposition and collaborative filtering in the informatics science field.

Here, we describe the identification of highly orally active fXa inhibitors based on our conjugation strategy and retrospective application of our newly developed fragment recommender system.

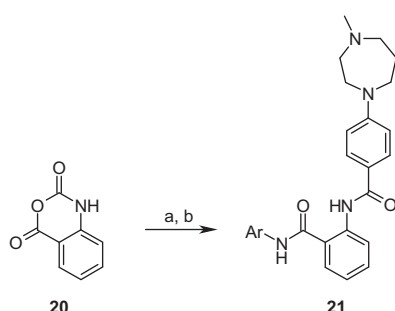
## 2. Inhibitor design

To identify novel potent and orally-active inhibitors of fXa, we adopted our previously reported conjugation strategy.<sup>19</sup> Exploration of orally efficacious inhibitors based on this methodology consists of two steps.

The first step is search for a suitable template inhibitor and the identification of an appropriate position for the introduction of a phenolic hydroxyl group into the inhibitor. Figure 1 depicts the structures of compound **1** and its active glucuronide conjugate **2** (YM-222714).<sup>18</sup> We previously reported that the 3-position of the central phenyl ring of compounds **1** and **2** pointed towards solvent-exposed region, and the sugar residue of compound **2** was projected out from the enzyme active site into the bulk solvent. We also identified the related anthranilamide analogue **3**.<sup>18</sup> The high structural similarity between compounds **1** and **3** convinced



**Scheme 2.** (a) *N*-Chlorosuccinimide, DMF, 50 °C; (b) HCl aq, reflux; (c) ArNH<sub>2</sub>, 1-hydroxybenzotriazole, 1-(3-dimethylaminopropyl)-3-ethylcarbodiimide hydrochloride, DMF; (d) Ar'COCl, pyridine.



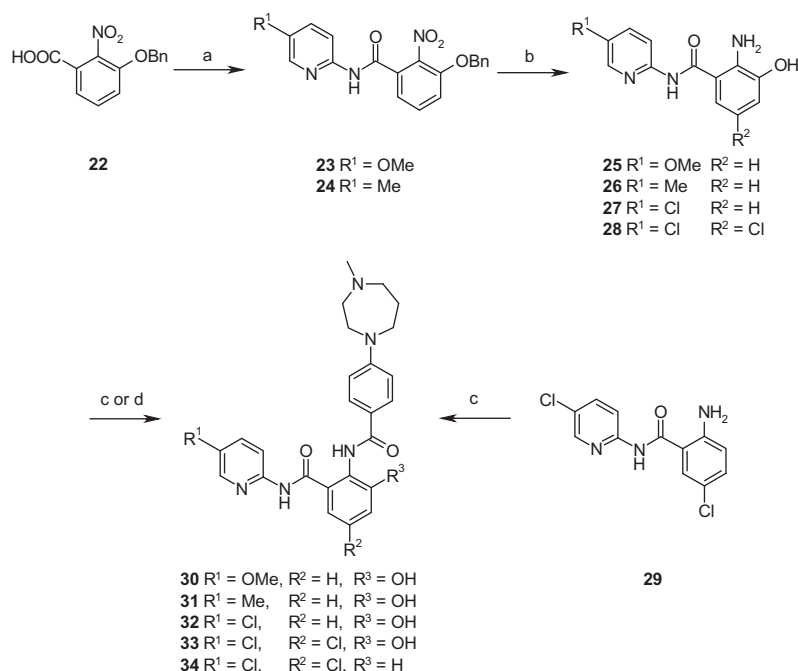
**Scheme 3.** (a) ArNH<sub>2</sub>, toluene, reflux; (b) Ar'COCl, pyridine.

us that the 3-position on the central phenyl ring of compound **3** would point toward the outside of the enzyme in the same way as that of compound **1** without direct interaction between the enzyme and a substituent on this position. We therefore selected the anthranilamide **3** as a template scaffold and planned to introduce a phenolic hydroxyl moiety on its 3-position in central ring.

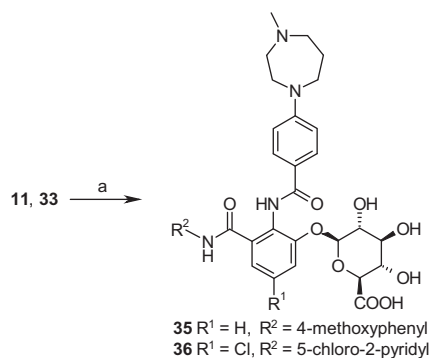
The next step is the optimization of chemical structures as enzyme inhibitors. We assumed that the overall interaction of a glucuronide-conjugated inhibitor with the enzyme is due to the aglycon unit because of the sugar residue being located in the solvent sphere, and that structural optimization of the aglycon could therefore result in improved inhibitory activity of the glucuronide-conjugated inhibitor. On the exploration of the structural modification, conformational maintenance of the aglycon should be important because conformational change would result in the sugar residue being located in an undesired orientation. We therefore focused our efforts on structural modifications of the distal anisidine and the central phenyl moieties of compound **3**.

### 3. Chemistry

Preparation of *N*<sup>1</sup>-phenylanthranilamide derivatives **11–14** is illustrated in Scheme 1. 2-Nitrobenzoic acids **4** and **5** were treated with appropriately substituted anilines in the presence of carbodiimide to yield benzanilide derivatives **6–9**. Reductions of their nitro groups were performed using two general procedures. Compound **6** was transformed to aniline by catalytic hydrogenation.



**Scheme 4.** (a) (i) Oxalyl chloride, cat.DMF, CH<sub>2</sub>Cl<sub>2</sub>; (ii) ArNH<sub>2</sub>, pyridine; (b) H<sub>2</sub>, 10% Pd-C, ethanol; (c) Ar'COCl, pyridine; (d) (i) Ar'COCl, pyridine; (ii) acetic acid, 60 °C.



**Scheme 5.** (a) (i) Acetobromo- $\alpha$ -D-glucuronic acid methyl ester, 1,8-diazabicyclo-[5.4.0]-7-undecene,  $CHCl_3$ , methanol; (ii)  $Na_2CO_3$ ,  $H_2O$ .

Alternatively, compounds **7–9** were converted to anilines by treatment with reduced iron and ammonium chloride. The intermediate anilines were acylated with acid chloride, which was prepared from 4-(4-methyl-1,4-diazepan-1-yl)benzoic acid hydrochloride (**10**),<sup>22</sup> to afford the desired  $N^1$ -phenylanthranilamide derivatives **11–14**.

Scheme 2 depicts the subsequent steps that were employed to elaborate compound **19**. Treatment of ethyl anthranilate **15**<sup>23</sup> with  $N$ -chlorosuccinimide provided its 5-chloro analogue **16** which was then hydrolyzed under acidic condition to give anthranilic acid **17**. Amide bond formation with  $p$ -anisidine followed by acylation with compound **10** provided the target compound **19**.

The library of anthranilamide derivatives were prepared by solution-phase parallel synthesis, which is outlined in Scheme 3. Coupling of isatoic anhydride with a collection of anilines followed by treatment with acid chloride gave a set of 57  $N^1$ -phenylanthranilamide derivatives **21**.

Preparation of a collection of  $N^1$ -(2-pyridyl)anthranilamide derivatives is shown in Scheme 4. 3-Benzyloxy-2-nitrobenzoic acid **22**<sup>24</sup> was converted to acid chloride by treatment with oxalyl chloride and then coupled with appropriately substituted aminopyridines to afford amides **23** and **24**. The methoxy and methyl-containing benzyloxynitrobenzenes **23** and **24** were

transformed into aminophenols **25** and **26** by one-step catalytic hydrogenation with palladium on carbon, respectively. Aminophenols **25**, **26**, and **27**<sup>19</sup> were reacted with acid chloride **10** to give the desired amides **30–32**. Analogous 5-chloro derivative **28**<sup>19</sup> was transformed into the target compound **33** via a two-step procedure involving acylation with acid chloride **10** and subsequent  $O$ - to  $N$ -migration of benzoyl moiety under acidic condition. Deshydroxy analogue **34** was prepared starting from previously reported aniline **29**.<sup>25</sup>

Phenol derivatives **11** and **33** were converted into the corresponding glucuronides **35** and **36**, respectively (Scheme 5). Treatment of phenols **11** and **33** with acetobromo- $\alpha$ -D-glucuronic acid methyl ester in the presence of 1,8-diazabicyclo-[5.4.0]-7-undecene followed by basic hydrolysis afforded the desired phenol glucuronides **35** and **36**, respectively. A  $^1H$  nuclear magnetic resonance (NMR) spectrum of compound **35** showed a signal at  $\delta = 4.95$  ppm with an axial-axial coupling of 7.8 Hz in agreement with its  $\beta$ -configuration of the anomeric position.<sup>26–28</sup> The structure of the  $\beta$ -configuration of compound **36** was also supported by an anomeric doublet at  $\delta = 5.06$  ppm with a coupling of 7.3 Hz characteristics of the expected axial-axial arrangement.

#### 4. Results and discussion

For all synthesized compounds, the inhibition of human fXa in a purified enzyme system was tested. For selected compounds, subsequent screening against human thrombin for selectivity within the coagulation cascade and human trypsin for general specificity against serine proteases was conducted. Prothrombin time (PT) prolongation effect was evaluated as an indicator of anticoagulant activity via oral dosing of the test compounds. FXa inhibitors were dosed to male ICR mice using gastric tube; 0.5 h after oral administration, blood was collected and platelet poor plasma was prepared to measure PT.

Table 1 shows the results of modification on the central core of compound **3**. As the high structural similarity between compounds **1** and **3** had suggested that the introduction of a substituent into the 3-position on the central phenyl ring of compound **3** would maintain fXa inhibitory activity, the phenol derivative **11** and its corresponding glucuronide **35** demonstrated comparable fXa

**Table 1**  
Effect of modification of central core

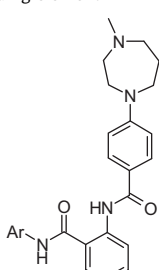
Compd	W	R	IC <sub>50</sub> <sup>a</sup> (μM) fXa	Prolongation effect <sup>b</sup> PT/control PT (fold)
<b>3</b>	H	H	0.14	1.02
<b>11</b>	OH	H	0.15	1.97
<b>35</b>	OGlu	H	0.066	NT <sup>c</sup>
<b>14</b>	OH	4-Me	0.061	0.95
<b>19</b>	OH	5-Cl	0.068	3.91
DPC423			0.0024	1.61

<sup>a</sup> Inhibitory activity against human purified enzyme. IC<sub>50</sub> value are represented by the average of three separate determinations with an average standard error of the mean of <20%.

<sup>b</sup> Relative prothrombin time (PT) compared with that measured using normal mice plasma at 0.5 h after oral administration (100 mg/kg,  $n = 3$ ). Each value are represented by the average with an average standard error of the mean of <20%.

<sup>c</sup> Not Tested.

**Table 2**  
Effect of modification of P1 binding element



Compd	Ar	Inh.% <sup>a</sup> fXa	Compd	Ar	Inh.% <sup>a</sup> fXa
<b>21a</b>		16	<b>21l</b>		24
<b>21b</b>		88	<b>21m</b>		15
<b>21c</b>		94	<b>21n</b>		23
<b>21d</b>		11	<b>21o</b>		38
<b>21e</b>		76	<b>21p</b>		73
<b>21f</b>		100	<b>21q</b>		9
<b>21g</b>		40	<b>21r</b>		56
<b>3</b>		85	<b>21s</b>		7
<b>21h</b>		NE <sup>b</sup>	<b>21t</b>		NE <sup>b</sup>
<b>21i</b>		39	<b>21u</b>		NE <sup>b</sup>
<b>21j</b>		32	<b>21v</b>		NE <sup>b</sup>
<b>21k</b>		22	<b>21w</b>		NE <sup>b</sup>

<sup>a</sup> Inhibitory activity against human purified fXa. Inhibition% means anti-fXa activity at a final inhibitor concentration of 1.36  $\mu$ M. The values are determined by a single experimental run.

<sup>b</sup> No effect.

inhibitory activity to the parent inhibitor **3** (IC<sub>50</sub>; 150 and 66 nM, respectively). The phenol **11** exhibited improved oral anticoagulant activity compared to the deshydroxy parent **3**, which convinced us that our conjugation strategy was applicable to the discovery program for orally active anticoagulants based on compound **3**. Although 4-methyl-3-hydroxy analogue **14** did exhibit equipotent in vitro anti-fXa activity to the 3-hydroxy derivative **11**, it did not exhibit PT-prolongation effect after oral administration. Confirmation with a parallel artificial membrane permeability assay (PAMPA) demonstrated comparable permeability of compounds **11** and **14** ( $>30 \times 10^{-6}$  cm/s). Sterically blocked phenols are less reactive in glucuronide-conjugation compared than less hindered phenols,<sup>29–31</sup> suggesting that substitution in the neighborhood of the phenolic hydroxyl group interfered with conjugation and caused a significant loss of oral anticoagulant activity.

Our efforts next focused to the further optimization step of the aglycon. An anthranilamide scaffold with a chloro substituent at the 5-position in the central phenyl core is a well-known motif for fXa inhibitors,<sup>19,32</sup> which encouraged us to install a 5-chloro group on the central ring of our inhibitor **11**. This installation resulted in compound **19** demonstrating enhanced fXa inhibition and potent anticoagulant activity with a PT-prolongation value of 3.9-fold after oral administration.

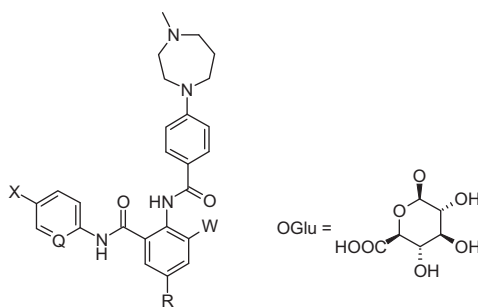
To identify surrogates for the *p*-anisidine moiety, we adopted a rapid search with parallel synthesis methodology to prepare over 50 analogues of the lead compound **3**. Table 2 demonstrates the assay results for a representative set of compounds. The structure–activity relationships (SARs) in this region were summarized as follows: (1) 4-substituted phenyl derivatives demonstrated potent inhibitory activity against fXa compared to the corresponding 2- or 3-substituted phenyl analogues, (2) a small lipophilic group, such as chloro, methyl, or methoxy, at the 4-position on the phenyl moiety exhibited potent inhibitory activity, but bulkier substituents at this position were deleterious, (3) transformation into 2-aminopyridine was tolerated, but compounds with other cyclic systems, such as 3-aminopyridines, 5-membered ring systems, or bicyclic ring systems, were poor fXa inhibitors. Given these results, we planned to concentrate our efforts on further investigation of *p*-anisidine, *p*-toluidine, *p*-chloroaniline, and their matched molecular pairs of 5-substituted 2-aminopyridines as the P1 binding elements.

The results of replacing the *p*-anisidine group of compound **11** with the selected motifs described above are shown in Table 3. Substitution with *p*-toluidine (**12**) maintained the fXa inhibitory activity, and the *p*-chloroaniline derivative **13** was a highly potent fXa inhibitor with an IC<sub>50</sub> value of 6.9 nM. These two phenols demonstrated potent PT-prolongation effect after oral dosing, and higher ex vivo anticoagulant effect was observed with an improvement in in vitro anti-fXa activity of aglycon. The 2-aminopyridine derivatives **30**, **31**, and **32** demonstrated slightly reduced fXa inhibitory activity compared to the corresponding phenyl pairs **11**, **12**, and **13**, respectively. However, the 2-aminopyridine series demonstrated a more potent anticoagulant effect via oral dosing than the corresponding phenyl series. The SAR trend in this anthranilamide series was different from the SAR spectrum of our previous phenylenediamine derivatives, in which only compounds with a methoxy group on the distal aromatic ring showed a potent oral anticoagulant effect.<sup>18</sup> We concluded that 5-chloro-2-aminopyridyl unit was the optimal fragment for enhancement of the ex vivo anticoagulant effect in this series.

Our SAR analysis and intuitive perspective prompted us to prepare a novel aglycon with a combination of a chloro-substituent on the 5-position of the central ring and a 5-chloro-2-aminopyridine unit as the P1 element, in expectation of boosting oral activity. Synthesized compound **33** was a potent fXa inhibitor with an IC<sub>50</sub> value of 8.7 nM and also an excellent orally-active anticoagulant with 7.8-fold PT-prolongation effect (Table 3). The corresponding deshydroxy analogue **34** did not demonstrate oral activity despite its comparable in vitro fXa inhibitory activity to compound **33**, reconfirming that the phenolic hydroxyl group was essential to boost oral anticoagulant effect. The corresponding glucuronide **36** displayed an approximately 20-fold increase in fXa inhibitory activity over glucuronide **35**, a similar improvement in activity to that observed in the aglycons **33** and **11**. These results were consistent with our initial hypothesis that structural optimization of an aglycon, which would interact with the active site of the enzyme, would result in an improvement in enzymatic inhibitory activity of the corresponding glucuronide-conjugated inhibitor.

The phenol **33** and its glucuronide conjugate **36** were selected for further evaluation in our advanced profiling assays. Compound **33** exhibited dose-dependent anticoagulant activity following oral

**Table 3**  
Effect of modification of central core and P1 binding element



Compd	W	R	X	Q	IC <sub>50</sub> <sup>a</sup> (μM) fXa	Prolongation effect <sup>a</sup> PT/control PT (fold)
<b>11</b>	OH	H	OMe	CH	0.15	1.97
<b>12</b>	OH	H	Me	CH	0.068	2.11
<b>13</b>	OH	H	Cl	CH	0.0069	2.67
<b>30</b>	OH	H	OMe	N	0.22	2.03
<b>31</b>	OH	H	Me	N	0.29	2.13
<b>32</b>	OH	H	Cl	N	0.016	3.61
<b>33</b>	OH	Cl	Cl	N	0.0087	7.80
<b>34</b>	H	Cl	Cl	N	0.0036	1.21
<b>36</b>	OGlu	Cl	Cl	N	0.0015	NT <sup>a</sup>
DPC423					0.0024	1.61

<sup>a</sup> See the corresponding footnotes in Table 1.

**Table 4**  
In vitro inhibitory activities and anticoagulant activities

Compd	IC <sub>50</sub> <sup>a</sup> (μM)			CT <sub>2</sub> <sup>b</sup> (μM) PT <sup>c</sup>	
	fXa	Thrombin	Trypsin	Human	Mouse
<b>36</b>	0.0015	>100	>100	0.27	0.28
DPC423	0.0024	>100	>100	0.67	0.70

<sup>a</sup> See the corresponding footnotes of Table 1.

<sup>b</sup> CT<sub>2</sub> values are defined as the concentration required to double clotting time and represent the average of three separate determinations with the average standard errors of the mean being <10%.

<sup>c</sup> Prothrombin time.

administration, and demonstrated over 10 times more potency in PT-prolongation effect than DPC423, the clinical candidate as an antithrombotic agent at the time of our study (Fig. 4). Pharmacokinetic evaluation revealed that conjugation to the corresponding glucuronide was observed when compound **33** was dosed orally, and that plasma concentration of the parent phenol **33** was below the limit of quantification (data not shown). Subsequent screening against human thrombin for selectivity within the coagulation cascade and human trypsin for general specificity against serine proteases, as well as in vitro anticoagulant activities in human and mice plasma was carried out for the potent fXa inhibitor **36** (Table 4). Compound **36** exhibited highly selectivity for both thrombin and trypsin (>10,000-fold), and also showed potent in vitro PT-prolongation activity. These results indicated that glucuronide **36** demonstrated ex vivo PT-prolongation effect due to its specific fXa inhibitory activity after oral dosing of the phenol **33**.

## 5. Fragment recommender system

For structural optimization process, we developed a novel interpretable and predictable compound design workflow that recommends promising fragments on the basis of common scaffold detection, R-group decomposition, and recommender system in the informatics science field.<sup>33</sup> In this section, we describe the concept and retrospective application to our exploratory study.

The first step is the preparation of 'Fragment Matrices' via common scaffold detection and following R-group decomposition for target sets of compounds. Figure 2 shows a brief example of our concept for restructuring SAR information. SAR analysis is a general process in drug discovery research, in which almost all medicinal chemists utilize SAR tables. The first step for preparation of fragment matrices involves transforming SAR tables to matrices in which rows corresponded to scaffolds and columns to substituents. Both rows and columns are then ordered by hierarchical

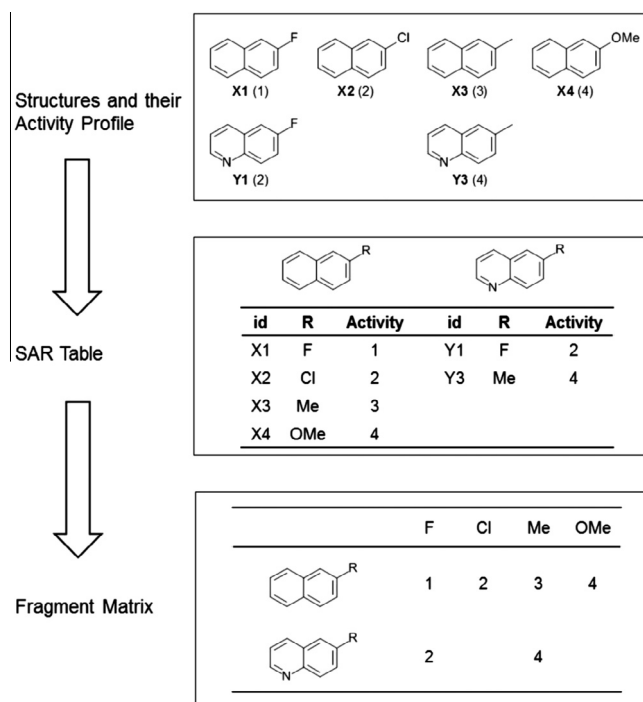


**Figure 2.** Conceptual example of restructuring SARs information. Figures in parentheses of the top box represent hypothetical activity.



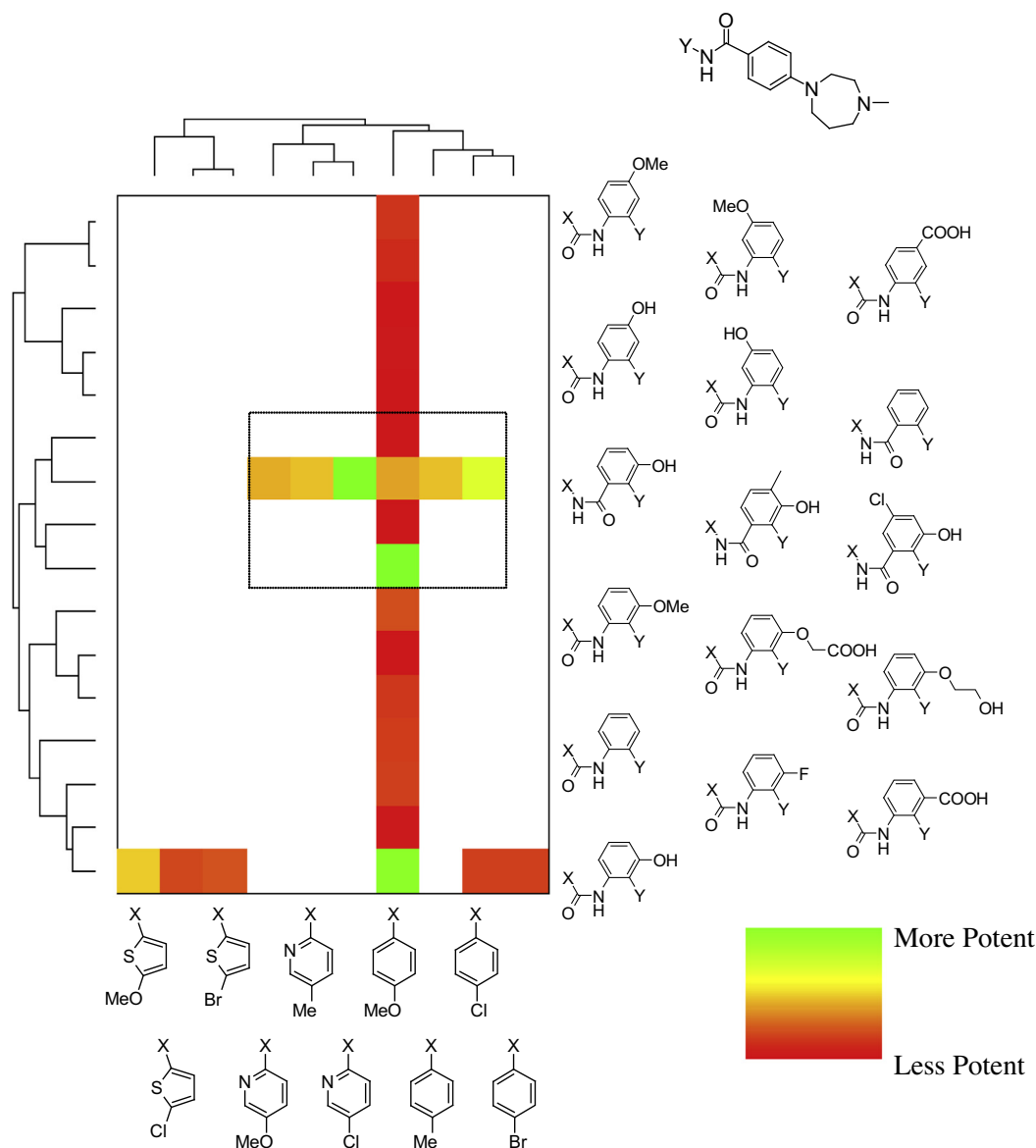


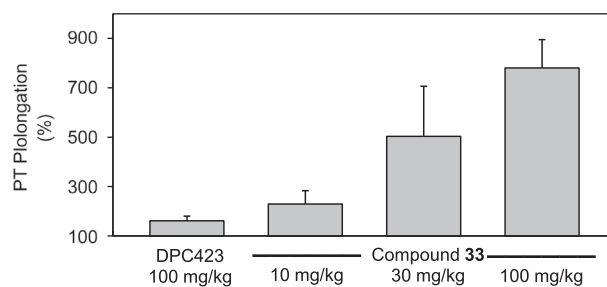
**Figure 3.** Fragment matrix for oral anticoagulant effect.

clustering based on structural similarity, and dendrograms are arranged in the outer area of the matrix to resemble a heatmap. Intersections of rows and columns, namely a combination of a scaffold and a substituent, equals one compound, and its similar analogues are located in the neighborhood in this fragment matrix. Bajorath et al. pioneered the visualization of SARs and recently they reported a relative workflow.<sup>34,35</sup>

The second step is quantitative estimation based on a similar concept to Free-Wilson analysis.<sup>20,21</sup> This analysis and traditional SAR study by medicinal chemists estimates the changes in biological activities or physicochemical properties as a linear combination of the effects of modification of scaffolds and substituents. Analogical estimation of the activity or property of a newly designed compound could therefore be well-implemented by linear regression of substituent transformation with the relative weighting of scaffold similarity. In the case of the previous instance, 6-chloro and 6-methoxyquinoline would be estimated to show activity values of 3 and 5, respectively. This is the same concept as collaborative filtering of recommender system in the informatics science field. Therefore, the integration of fragment

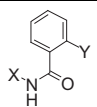
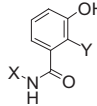
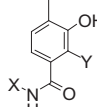
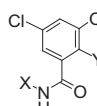
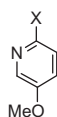
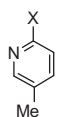
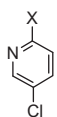
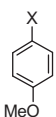
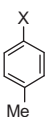
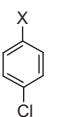
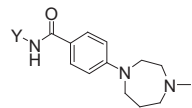
matrices with collaborative filtering functions into our fragment recommender system that thereby enables novel interpretation and prediction of promising substituents.

Here, we first explored SARs around the central core and P1 binding element and then investigated their combination effect.



**Figure 4.** Anticoagulant activity of compound **33** 0.5 h after oral dosing in mice. Relative prothrombin time (PT) compared to that measured using normal mice plasma (mean + standard deviation,  $n = 3$ ).

**Table 5**  
Measured and simulated oral anticoagulant effect by slope one estimation<sup>a</sup>

(1.00)	(1.02)	(1.05)	1.02	(1.02)	(1.03)	
2.03	2.13	3.61	1.97	2.11	2.67	
(1.00)	(1.00)	(1.00)	0.95	(1.00)	(1.00)	
(4.09)	(4.39)	(8.83)	3.91	(4.33)	(6.01)	
						

<sup>a</sup> Figures in parentheses represent estimated values.

For retrospective application of our fragment recommender system design workflow, we selected the combination step as a case study. We used a collection of diazepane derivatives **1**, **3**, **11–14**, **19**, **30–32** and additional 16 analogues described in our previous work as a training set.<sup>18</sup> Figure 3 shows this set of compounds tabled in a fragment matrix in which columns corresponded P1 binding elements and rows to scaffolds. To grasp SARs instantly, this matrix visualizes compound potency with colored cells that range from red for low potency to green for high potency. This diagram promptly highlights important SARs. The scaffolds are classified into three groups, as follows: 4- and 5-substituted phenylenediamine scaffold (rows 1–5), 3-substituted anthranilamide (rows 6–9, enclosed in the dotted box), and 3-substituted phenylenediamine (rows 10–16). The compounds in the second group frequently demonstrate higher activity than the others, and the SARs around P1 elements of second group differ from those of the third one. These observations are consistent with our findings by traditional SAR analysis.

Our focus on the second group with the aim of boosting oral activity led us to estimate values of blank cells, namely to predict the activity of practicable compounds. Slope One algorithm<sup>36</sup> used for collaborative filtering for the second cluster afforded an all-filled matrix (Table 5) and recommended a compound with a combination of chloro-substituent on the 5-position of the central ring and 5-chloro-2-aminopyridine for the P1 element as the most potent compound, with an estimated PT-prolongation value of 8.8-fold. The proposed compound was closely to compound **33**, as were the estimated and measured activities.

## 6. Conclusion

We designed and synthesized a series of novel orally active fXa inhibitors based on our conjugation strategy. Our previously reported fXa inhibitor **3** was selected as a lead compound. The high structural similarity between compounds **1** and **3** led us to select substitution point for introduction of a sugar residue, which afforded a glucuronide-conjugated fXa inhibitor **35** with comparable in vitro inhibitory activity to compound **3**. The corresponding

phenol **11** demonstrated enhanced anticoagulant activity compared to the parent deshydroxy analogue **3** after oral administration. Based on our hypothesis that an interaction of a glucuronide-conjugated inhibitor with the active site of the enzyme would be formed by its aglycon and that structural optimization of the aglycon could improve the inhibitory activity of the conjugated inhibitor, we conducted structural modifications of compound **11**. Our efforts to focus on the central phenyl ring and the P1 binding element culminated in the identification of compound **33** (AS1468240), which exhibited potent fXa inhibitory activity and excellent PT-prolongation effect when administered orally.

We also developed a new Free-Wilson-like fragment recommender system for the interpretation and prediction in the compound design process based on an integration of common scaffold detection, R-group decomposition, and collaborative filtering. We retrospectively applied this workflow to our study, which afforded computational analytical results that were consistent with our findings by traditional SAR analysis and recommended a combination of fragments for a promising candidate. The details of our newly developed fragment recommender system will be published in due course.

## 7. Experimental

### 7.1. Chemistry

<sup>1</sup>H NMR spectra were measured with a JEOL JNM-LA300 or JEOL EX400 spectrometer. Chemical shifts are expressed in  $\delta$  units using tetramethylsilane as the standard (in the NMR description, s = singlet, d = doublet, t = triplet, m = multiplet, and br = broad peak). Mass spectra were recorded on a JEOL JMS-LX2000 spectrometer. For salts, assignments of ion peaks are based on the basic component. The elemental analyses were performed with a Yanaco MT-5 microanalyzer (C, H, and N) and a Yokogawa IC-7000S ion chromatographic analyzer (Cl). Melting points were measured using a Yanaco MP-500D melting point apparatus without correction. All reagents purchased were used without further purification. C-18 reversed-phase silica gel (ODS) column chromatography was performed on YMC gel (ODS-A 120–230/70).



### 7.1.1. 3-Hydroxy-4'-methoxy-2-nitrobenzanilide (6)

To a stirred solution of 3-hydroxy-2-nitrobenzoic acid (**4**) (1.83 g, 10.0 mmol), *p*-anisidine (1.23 g, 10.0 mmol), and 1-hydroxybenzotriazole hydrate (1.35 g, 10.0 mmol) in 20 mL of *N,N*-dimethylformamide (DMF) was added 1-[3-(dimethylamino)propyl]-3-ethylcarbodiimide hydrochloride (2.50 g, 13.0 mmol) at ambient temperature. After 3 days, the reaction mixture was concentrated in vacuo. The residue was diluted with ethyl acetate and washed with H<sub>2</sub>O. The organic layer was dried over magnesium sulfate and concentrated in vacuo. The residue was triturated with CHCl<sub>3</sub> and the resulting solid was filtered off to yield the title compound as a colorless solid (2.04 g, 71%); mp 180–181 °C; <sup>1</sup>H NMR (300 MHz, DMSO-*d*<sub>6</sub>) δ 3.74 (3H, s), 6.92 (2H, d, *J* = 8.8 Hz), 7.21–7.26 (2H, m), 7.50 (1H, t, *J* = 8.6 Hz), 7.58 (2H, d, *J* = 8.8 Hz), 10.45 (1H, s), 11.20 (1H, br s); FAB-MS *m/z* 289 [M+H]<sup>+</sup>.

### 7.1.2. 3-Hydroxy-4'-methoxy-2-[[4-(4-methyl-1,4-diazepan-1-yl)benzoyl]amino]benzanilide Hydrochloride (11)

To a mixture of compound **6** (1.15 g, 4.00 mmol) and methanol (50 mL) was added 10% Pd-C (300 mg) and the whole was stirred under hydrogen at atmospheric pressure for 1 h. The reaction mixture was filtered through a pad of Celite® and concentrated in vacuo to yield 966 mg of 2-amino-3-hydroxy-4'-methoxybenzanilide (966 mg, 94%). The resulting material was used in subsequent reactions without purification. A mixture of compound **10**<sup>22</sup> (812 mg, 3.00 mmol) and thionyl chloride (8.0 mL) was stirred at 60 °C for 30 min. The reaction mixture was concentrated in vacuo to yield 4-(4-methyl-1,4-diazepan-1-yl)benzoyl chloride hydrochloride (**37**). This material and 2-amino-3-hydroxy-4'-methoxybenzanilide (774 mg) were combined in pyridine (15 mL) and the whole was stirred at ambient temperature for 2 h. The reaction mixture was concentrated in vacuo. The residue was diluted with ethyl acetate and washed with 5% aqueous sodium bicarbonate. The resulting precipitate was filtered off. The organic layer was dried over magnesium sulfate and concentrated in vacuo. The residue was combined with the filtrate described above, and the whole was subjected to chromatography over silica gel eluting with CHCl<sub>3</sub>/MeOH (95:5 by volume). The resulting material was suspended in EtOH (10 mL). To this suspension was added 4 N hydrogen chloride in ethyl acetate (0.7 mL) and the whole was stirred for 0.5 h. The resulting precipitate was filtered off and dried in vacuo to yield the title compound as a pale yellow solid (896 mg, 58%); mp 169–171 °C; <sup>1</sup>H NMR (400 MHz, DMSO-*d*<sub>6</sub>) δ 2.10–2.41 (2H, m), 2.78 (3H, s), 3.02–3.22 (2H, m), 3.35–3.57 (4H, m), 3.67–3.81 (4H, m), 3.87–3.99 (1H, m), 6.80–6.95 (4H, m), 7.11 (1H, d, *J* = 7.3 Hz), 7.17–7.28 (2H, m), 7.57 (2H, d, *J* = 8.8 Hz), 7.85 (2H, d, *J* = 8.8 Hz), 10.02 (1H, s), 10.19 (1H, s), 10.41 (1H, s), 10.64 (1H, br s); FAB-MS *m/z* 475 [M+H]<sup>+</sup>; Anal. calcd for C<sub>27</sub>H<sub>30</sub>N<sub>4</sub>O<sub>4</sub>·HCl·H<sub>2</sub>O: C, 61.30; H, 6.29; N, 10.59; Cl, 6.70. Found: C, 61.37; H, 6.47; N, 10.33; Cl, 6.59.

### 7.1.3. 4'-Chloro-3-hydroxy-2-nitrobenzanilide (8)

To a stirred solution of compound **4** (2.00 g, 10.9 mmol), 4-chloroaniline (1.53 g, 12.0 mmol), and 1-hydroxybenzotriazole hydrate (2.21 g, 16.4 mmol) in DMF (100 mL) was added 1-[3-(dimethylamino)propyl]-3-ethylcarbodiimide hydrochloride (3.15 g, 16.4 mmol) at ambient temperature. After 2 days, the reaction mixture was concentrated in vacuo. The residue was diluted with CHCl<sub>3</sub> and washed with brine. The organic layer was dried over magnesium sulfate and concentrated in vacuo. The residue was subjected to chromatography over silica gel eluting with CHCl<sub>3</sub>/MeOH (100:1 by volume) to yield the title compound as a beige amorphous powder (2.97 g, 93%); <sup>1</sup>H NMR (300 MHz, CDCl<sub>3</sub>) δ 7.08 (1H, dd, *J* = 1.1 and 7.1 Hz), 7.26 (1H, dd, *J* = 1.1 and 8.6 Hz), 7.34 (2H, d, *J* = 8.6 Hz), 7.53–7.62 (3H, m), 7.97 (1H, s), 10.48 (1H, br s); FAB-MS *m/z* 293 [M+H]<sup>+</sup>.

### 7.1.4. 4'-Chloro-3-hydroxy-2-[[4-(4-methyl-1,4-diazepan-1-yl)benzoyl]amino]benzanilide Hydrochloride (13)

A mixture of compound **8** (1.43 g, 4.89 mmol), reduced iron (2.80 g, 49.0 mmol), ammonium chloride (2.80 g, 49.0 mmol), methanol (50 mL), and H<sub>2</sub>O (5 mL) was stirred at 60 °C for 3 h. The reaction mixture was filtered through a pad of Celite® and concentrated in vacuo. The residue was subjected to chromatography over silica gel eluting with *n*-hexane/ethyl acetate (1:1 by volume) to yield 2-amino-4'-chloro-3-hydroxybenzanilide (270 mg, 21%). To a stirred solution of 2-amino-4'-chloro-3-hydroxybenzanilide (270 mg, 1.03 mmol) in pyridine (11 mL) was added compound **37** (447 mg, 1.55 mmol). After 2 days, the reaction mixture was concentrated in vacuo. The residue was diluted with CHCl<sub>3</sub> and washed with 5% aqueous sodium bicarbonate. The organic layer was dried over magnesium sulfate and concentrated in vacuo. The residue was subjected to chromatography over silica gel eluting with CHCl<sub>3</sub>/MeOH/*c*.NH<sub>3</sub> (100:5:0.5 by volume). The resulting material was dissolved in EtOH (7.3 mL). To this solution was added 1 N hydrochloric acid (1.1 mL), and the whole was stirred for 0.5 h. The resulting precipitate was filtered off and dried to yield the title compound as a colorless solid (299 mg, 56%); mp 197–199 °C; <sup>1</sup>H NMR (400 MHz, DMSO-*d*<sub>6</sub>) δ 2.12–2.21 (1H, m), 2.26–2.39 (1H, m), 2.78 (3H, s), 3.03–3.20 (2H, m), 3.30–3.54 (4H, m), 3.72–3.78 (1H, m), 3.89–3.96 (1H, m), 6.84 (2H, d, *J* = 8.8 Hz), 7.10–7.13 (1H, m), 7.15–7.18 (1H, m), 7.22–7.26 (1H, m), 7.36 (2H, d, *J* = 8.8 Hz), 7.71 (2H, d, *J* = 8.8 Hz), 7.85 (2H, d, *J* = 8.8 Hz), 9.96 (1H, s), 9.99 (1H, s), 10.40 (1H, s), 10.76 (1H, br s); FAB-MS *m/z* 479 [M+H]<sup>+</sup>; Anal. calcd for C<sub>26</sub>H<sub>27</sub>N<sub>4</sub>O<sub>3</sub>Cl·0.9HCl·0.5H<sub>2</sub>O: C, 59.96; H, 5.59; N, 10.76; Cl, 12.93. Found: C, 59.66; H, 5.95; N, 9.94; Cl, 12.74.

### 7.1.5. 3-Hydroxy-4'-methyl-2-nitrobenzanilide (7)

The title compound was obtained from *p*-toluidine using the methods described for the synthesis of compound **8** as a beige amorphous powder (quant); <sup>1</sup>H NMR (300 MHz, CDCl<sub>3</sub>) δ 2.35 (3H, s), 7.09 (1H, dd, *J* = 1.3 and 7.3 Hz), 7.19 (2H, d, *J* = 8.1 Hz), 7.26 (1H, dd, *J* = 1.3 and 8.4 Hz), 7.47 (2H, d, *J* = 8.1 Hz), 7.57–7.62 (1H, m), 8.00 (1H, s), 10.49 (1H, s); FAB-MS *m/z* 273 [M+H]<sup>+</sup>.

### 7.1.6. 3-Hydroxy-4'-methyl-2-[[4-(4-methyl-1,4-diazepan-1-yl)benzoyl]amino]benzanilide Hydrochloride (12)

The title compound was obtained from compound **7** using the methods described for the synthesis of compound **13** as a colorless solid (12%); mp 216–217 °C; <sup>1</sup>H NMR (400 MHz, DMSO-*d*<sub>6</sub>) δ 2.08–2.36 (5H, m), 2.78 (3H, s), 3.03–3.20 (2H, m), 3.32–3.54 (4H, m), 3.70–3.78 (1H, m), 3.89–3.96 (1H, m), 6.86 (2H, d, *J* = 8.8 Hz), 7.09–7.12 (3H, m), 7.18–7.26 (2H, m), 7.54 (2H, d, *J* = 8.8 Hz), 7.85 (2H, d, *J* = 9.3 Hz), 10.00 (1H, s), 10.20 (1H, s), 10.27 (1H, s), 10.64 (1H, br s); FAB-MS *m/z* 459 [M+H]<sup>+</sup>; Anal. calcd for C<sub>27</sub>H<sub>30</sub>N<sub>4</sub>O<sub>3</sub>·0.9HCl·H<sub>2</sub>O: C, 63.66; H, 6.51; N, 11.00; Cl, 6.26. Found: C, 63.99; H, 6.67; N, 10.35; Cl, 6.57.

### 7.1.7. 3-Hydroxy-4'-methoxy-4-methyl-2-nitrobenzanilide (9)

The title compound was obtained from 3-hydroxy-4-methyl-2-nitrobenzoic acid (**5**) using the methods described for the synthesis of compound **8** as a beige amorphous powder (79%); <sup>1</sup>H NMR (300 MHz, CDCl<sub>3</sub>) δ 2.36 (3H, s), 3.82 (3H, s), 6.92 (2H, d, *J* = 9.0 Hz), 7.00 (1H, d, *J* = 7.5 Hz), 7.35 (1H, br s), 7.45 (1H, d, *J* = 7.5 Hz), 7.50 (2H, d, *J* = 9.0 Hz); FAB-MS *m/z* 303 [M+H]<sup>+</sup>.

### 7.1.8. 3-Hydroxy-4'-methoxy-4-methyl-2-[[4-(4-methyl-1,4-diazepan-1-yl)benzoyl]amino]benzanilide Hydrochloride (14)

The title compound was obtained from compound **9** using the methods described for the synthesis of compound **13** as a colorless solid (24%); mp 259–261 °C; <sup>1</sup>H NMR (400 MHz, DMSO-*d*<sub>6</sub>) δ 2.11–2.21 (1H, m), 2.27–2.38 (4H, m), 2.78 (3H, s), 3.04–3.22 (2H, m),

3.38–3.56 (4H, m), 3.74–3.80 (4H, m), 3.91–3.99 (1H, m), 6.90–6.94 (4H, m), 7.18 (1H, d,  $J = 7.8$  Hz), 7.29 (1H, d,  $J = 7.8$  Hz), 7.59 (2H, d,  $J = 8.8$  Hz), 7.86 (2H, d,  $J = 9.3$  Hz), 10.11 (1H, s), 10.35 (1H, s), 10.72 (1H, br s), 11.42 (1H, s); FAB-MS  $m/z$  489 [M+H]<sup>+</sup>; Anal. calcd for C<sub>28</sub>H<sub>32</sub>N<sub>4</sub>O<sub>4</sub>·HCl·0.2H<sub>2</sub>O: C, 63.62; H, 6.37; N, 10.60; Cl, 6.71. Found: C, 63.57; H, 6.42; N, 10.54; Cl, 6.67.

#### 7.1.9. Ethyl 2-Amino-5-chloro-3-hydroxybenzoate (16)

A mixture of ethyl 2-amino-3-hydroxybenzoate (**15**)<sup>23</sup> (7.02 g, 38.8 mmol), *N*-chlorosuccinimide (5.18 g, 38.8 mmol), and DMF (50 mL) was stirred at 50 °C for 1.5 h. The reaction mixture was cooled to ambient temperature. The mixture was diluted with ethyl acetate and washed with 5% aqueous sodium bicarbonate, H<sub>2</sub>O, and then brine. The organic layer was dried over magnesium sulfate and concentrated in vacuo. The residue was dissolved in EtOH, decolorized with activated charcoal, filtered through a pad of Celite®, and concentrated in vacuo. The resulting solid was crystallized from EtOH/H<sub>2</sub>O to yield the title compound as a brown solid (7.92 g, 95%); mp 121–122 °C; <sup>1</sup>H NMR (300 MHz, CDCl<sub>3</sub>)  $\delta$  1.38 (3H, t,  $J = 7.3$  Hz), 4.33 (2H, q,  $J = 7.3$  Hz), 5.26 (1H, br s), 5.87 (2H, br s), 6.81 (1H, d,  $J = 2.4$  Hz), 7.48 (1H, d,  $J = 2.4$  Hz); FAB-MS  $m/z$  216 [M+H]<sup>+</sup>.

#### 7.1.10. 2-Amino-5-chloro-3-hydroxybenzoic Acid (17)

A mixture of compound **16** (3.23 g, 15.0 mmol) and 3 N hydrochloric acid (160 mL) was stirred at 80 °C for 5 days. The reaction mixture was cooled to ambient temperature and filtered. To the filtrate was added 1 N aqueous NaOH (320 mL) and the whole was stirred for 1 h. The resulting precipitate was filtered off, washed with H<sub>2</sub>O, and dried in vacuo to yield the title compound as a beige solid (1.55 g, 55%); mp >300 °C (dec); <sup>1</sup>H NMR (400 MHz, DMSO-*d*<sub>6</sub>)  $\delta$  3.37 (2H, br s), 6.78 (1H, d,  $J = 2.4$  Hz), 7.17 (1H, d,  $J = 2.4$  Hz), 8.34 (1H, br s), 10.19 (1H, s); FAB-MS  $m/z$  186 [M–H]<sup>+</sup>.

#### 7.1.11. 2-Amino-5-chloro-3-hydroxy-4'-methoxybenzanilide (18)

The title compound was obtained from compound **17** using the methods described for the synthesis of compound **6** as a brown solid (55%); mp 215–217 °C; <sup>1</sup>H NMR (400 MHz, DMSO-*d*<sub>6</sub>)  $\delta$  3.74 (3H, s), 5.93 (2H, br s), 6.78 (1H, d,  $J = 2.5$  Hz), 6.91 (2H, d,  $J = 9.3$  Hz), 7.23 (1H, d,  $J = 2.5$  Hz), 7.59 (2H, d,  $J = 9.3$  Hz), 9.90 (1H, s), 10.09 (1H, br s); FAB-MS  $m/z$  293 [M+H]<sup>+</sup>.

#### 7.1.12. 5-Chloro-3-hydroxy-4'-methoxy-2-[[4-(4-methyl-1,4-diazepan-1-yl)benzoyl]amino]benzanilide hydrochloride (19)

To a stirred solution of compound **18** (430 mg, 1.47 mmol) in pyridine (10 mL) was added compound **37** (577 mg, 2.00 mmol). After 24 h, the reaction mixture was concentrated in vacuo. The residue was diluted with CHCl<sub>3</sub> and washed with 5% aqueous sodium bicarbonate. The organic layer was dried over magnesium sulfate and concentrated in vacuo. The residue was subjected to chromatography over silica gel eluting with CHCl<sub>3</sub>/MeOH (100:5 by volume). The resulting material was dissolved in EtOH (10 mL) and added 1 N hydrochloric acid (0.8 mL), and the whole was stirred for 0.5 h. The resulting precipitate was filtered off and dried to yield the title compound as a colorless solid (250 mg, 31%); mp 248–251 °C; <sup>1</sup>H NMR (400 MHz, DMSO-*d*<sub>6</sub>)  $\delta$  2.10–2.34 (2H, m), 2.81 (3H, s), 3.01–3.25 (2H, m), 3.35–3.60 (4H, m), 3.62–3.79 (4H, m), 3.82–4.00 (1H, m), 6.84 (2H, d,  $J = 9.3$  Hz), 6.88 (2H, d,  $J = 8.8$  Hz), 7.12 (1H, d,  $J = 2.4$  Hz), 7.18 (1H, d,  $J = 2.4$  Hz), 7.54 (2H, d,  $J = 9.3$  Hz), 7.84 (2H, d,  $J = 8.8$  Hz), 9.86 (1H, br s), 9.96 (1H, s), 10.16 (1H, s), 10.43 (1H, s); ESI-MS  $m/z$  509 [M+H]<sup>+</sup>; Anal. calcd for C<sub>27</sub>H<sub>29</sub>N<sub>4</sub>O<sub>4</sub>Cl·0.9HCl·H<sub>2</sub>O: C, 57.93; H, 5.74; N, 10.01; Cl, 12.03. Found: C, 57.76; H, 5.38; N, 10.05; Cl, 12.05.

#### 7.1.13. Solution-phase synthesis of library compounds 21

Isoatoic anhydride (**20**) (0.1 mmol) was partitioned into reaction vials and treated with aniline (0.10 mmol) in toluene (1.0 mL) at 100 °C for 12 h. The mixture in each vessel was allowed to cool to ambient temperature, and the solvent was removed under reduced pressure. The residue in each vessel was dissolved in pyridine (1.0 mL) and treated with compound **37** (0.10 mol) at ambient temperature for 12 h. The mixture was then treated with polymer-bound tris(2-aminoethyl)amine for 12 h and filtered off. The filtrate was collected in vials and the solutions were evaporated in vacuo to afford anthranilamide derivatives **21**, which were analyzed by HPLC and MS. **21a**; FAB-MS  $m/z$  443 [M+H]<sup>+</sup>, **21b**; FAB-MS  $m/z$  443 [M+H]<sup>+</sup>, **21c**; FAB-MS  $m/z$  443 [M+H]<sup>+</sup>, **21d**; FAB-MS  $m/z$  463 [M+H]<sup>+</sup>, **21e**; FAB-MS  $m/z$  463 [M+H]<sup>+</sup>, **21g**; FAB-MS  $m/z$  459 [M+H]<sup>+</sup>, **21h**; FAB-MS  $m/z$  489 [M+H]<sup>+</sup>, **21i**; FAB-MS  $m/z$  493 [M+H]<sup>+</sup>, **21j**; FAB-MS  $m/z$  513 [M+H]<sup>+</sup>, **21k**; FAB-MS  $m/z$  521 [M+H]<sup>+</sup>, **21l**; FAB-MS  $m/z$  472 [M+H]<sup>+</sup>, **21m**; FAB-MS  $m/z$  457 [M+H]<sup>+</sup>, **21n**; FAB-MS  $m/z$  471 [M+H]<sup>+</sup>, **21o**; FAB-MS  $m/z$  430 [M+H]<sup>+</sup>, **21p**; FAB-MS  $m/z$  444 [M+H]<sup>+</sup>, **21q**; FAB-MS  $m/z$  444 [M+H]<sup>+</sup>, **21r**; FAB-MS  $m/z$  444 [M+H]<sup>+</sup>, **21s**; FAB-MS  $m/z$  460 [M+H]<sup>+</sup>, **21t**; FAB-MS  $m/z$  449 [M]<sup>+</sup>, **21u**; FAB-MS  $m/z$  433 [M+H]<sup>+</sup>, **21v**; FAB-MS  $m/z$  469 [M+H]<sup>+</sup>, **21w**; FAB-MS  $m/z$  480 [M+H]<sup>+</sup>. Compound **21f** was obtained from 2-amino-5-chloro-3-hydroxy-4'-methoxybenzanilide using the methods described for the synthesis of compound **19** as a colorless solid (423 mg, 56%); <sup>1</sup>H NMR (400 MHz, DMSO-*d*<sub>6</sub>)  $\delta$  2.15–2.25 (1H, m), 2.27–2.42 (1H, m), 2.78 (3H, d,  $J = 4.9$  Hz), 3.05–3.21 (2H, m), 3.39–3.56 (3H, m), 3.72–3.80 (1H, m), 3.90–4.06 (2H, m), 6.91 (2H, d,  $J = 9.3$  Hz), 7.22–7.26 (1H, m), 7.45 (2H, d,  $J = 8.7$  Hz), 7.57–7.62 (1H, m), 7.75–7.80 (4H, m), 7.93 (1H, d,  $J = 7.8$  Hz), 8.54 (1H, d,  $J = 8.3$  Hz), 10.68 (1H, s), 10.81 (1H, br s), 11.54 (1H, s); FAB-MS  $m/z$  463 [M+H]<sup>+</sup>.

#### 7.1.14. 3-Benzyloxy-*N*-(5-methoxy-2-pyridyl)-2-nitrobenzamide (23)

A mixture of 3-benzyloxy-2-nitrobenzoic acid (**22**)<sup>24</sup> (2.07 g, 7.57 mmol), three drops of DMF, and oxalyl chloride (1.92 g, 15.1 mmol) in CH<sub>2</sub>Cl<sub>2</sub> (33 mL) was stirred at ambient temperature for 3 h. The reaction mixture was concentrated in vacuo. This material and 2-amino-5-methoxypyridine (940 mg, 7.57 mmol)<sup>37</sup> were combined in pyridine (37 mL) and stirred at ambient temperature for 20 h. The reaction mixture was concentrated in vacuo. The residue was diluted with CHCl<sub>3</sub> and washed with 5% aqueous sodium bicarbonate. The organic layer was dried over magnesium sulfate and concentrated in vacuo. The residue was subjected to chromatography over silica gel eluting with CHCl<sub>3</sub>/MeOH (100:1 by volume) to give the title compound as a colorless amorphous powder (2.13 g, 74%); <sup>1</sup>H NMR (300 MHz, CDCl<sub>3</sub>)  $\delta$  3.84 (3H, s), 5.23 (2H, s), 7.19–7.49 (9H, m), 7.92 (1H, d,  $J = 2.9$  Hz), 8.22 (1H, d,  $J = 9.0$  Hz), 8.56 (1H, br s); FAB-MS  $m/z$  380 [M+H]<sup>+</sup>.

#### 7.1.15. 2-Amino-3-hydroxy-*N*-(5-methoxy-2-pyridyl)benzamide (25)

To a mixture of compound **23** (720 mg, 1.90 mmol) and methanol (19 mL) was added 10% Pd/C (70 mg) and the whole was stirred under hydrogen at 3 kgf/cm<sup>2</sup> for 1 h. The reaction mixture was filtered through a pad of Celite® and concentrated in vacuo to give the title compound as a brown amorphous powder (480 mg, 97%); <sup>1</sup>H NMR (300 MHz, DMSO-*d*<sub>6</sub>)  $\delta$  3.83 (3H, s), 5.89 (2H, br s), 6.43 (1H, t,  $J = 7.9$  Hz), 6.80 (1H, dd,  $J = 1.2$  and 7.9 Hz), 7.27 (1H, dd,  $J = 1.2$  and 7.9 Hz), 7.46 (1H, dd,  $J = 3.1$  and 9.2 Hz), 7.99 (1H, d,  $J = 9.2$  Hz), 8.08 (1H, d,  $J = 3.1$  Hz), 9.54 (1H, br s), 10.14 (1H, s); FAB-MS  $m/z$  260 [M+H]<sup>+</sup>.

**7.1.16. 3-Hydroxy-*N*-(5-methoxy-2-pyridyl)-2-[[4-(4-methyl-1,4-diazepan-1-yl)benzoyl]amino]benzamide Hydrochloride (30)**

The title compound was obtained from compound **25** using the methods described for the synthesis of compound **19** as a colorless solid (55%): mp 218–220 °C; <sup>1</sup>H NMR (400 MHz, DMSO-*d*<sub>6</sub>) δ 2.12–2.21 (1H, m), 2.29–2.41 (1H, m), 2.77 (3H, d, *J* = 4.9 Hz), 3.03–3.19 (2H, m), 3.36–3.82 (8H, m), 3.89–3.97 (1H, m), 6.84 (2H, d, *J* = 8.8 Hz), 7.11 (1H, dd, *J* = 2.4 and 6.8 Hz), 7.20–7.25 (2H, m), 7.45 (1H, dd, *J* = 2.9 and 9.3 Hz), 7.85 (2H, d, *J* = 8.8 Hz), 7.99–8.06 (2H, m), 9.98 (2H, s), 10.36 (1H, s), 10.92 (1H, br s); FAB-MS *m/z* 476 [M+H]<sup>+</sup>; Anal. calcd for C<sub>26</sub>H<sub>29</sub>N<sub>5</sub>O<sub>4</sub>·HCl·0.5H<sub>2</sub>O: C, 59.94; H, 6.00; N, 13.44; Cl, 6.80. Found: C, 59.77; H, 5.79; N, 13.41; Cl, 7.13.

**7.1.17. 3-Benzoyloxy-*N*-(5-methyl-2-pyridyl)-2-nitrobenzamide (24)**

The title compound was obtained from 2-amino-5-picoline using the methods described for the synthesis of compound **23** as a colorless amorphous powder (74%): <sup>1</sup>H NMR (400 MHz, CDCl<sub>3</sub>) δ 2.28 (3H, s), 5.23 (2H, s), 7.20–7.23 (1H, m), 7.26–7.28 (1H, m), 7.31–7.39 (5H, m), 7.45 (1H, t, *J* = 8.3 Hz), 7.56 (1H, dd, *J* = 2.5 and 8.8 Hz), 8.00 (1H, d, *J* = 2.5 Hz), 8.17 (1H, d, *J* = 8.8 Hz), 8.75 (1H, br s); FAB-MS *m/z* 364 [M+H]<sup>+</sup>.

**7.1.18. 2-Amino-3-hydroxy-*N*-(5-methyl-2-pyridyl)benzamide (26)**

The title compound was obtained from compound **24** using the methods described for the synthesis of compound **25** as a brown amorphous powder (87%): <sup>1</sup>H NMR (400 MHz, DMSO-*d*<sub>6</sub>) δ 2.27 (3H, s), 5.90 (2H, br s), 6.43 (1H, t, *J* = 8.0 Hz), 6.82 (1H, dd, *J* = 1.2 and 8.0 Hz), 7.27 (1H, dd, *J* = 1.2 and 8.0 Hz), 7.93 (1H, dd, *J* = 2.0 and 8.4 Hz), 7.99 (1H, d, *J* = 8.4 Hz), 8.19 (1H, d, *J* = 2.0 Hz), 9.56 (1H, br s), 10.16 (1H, s); FAB-MS *m/z* 244 [M+H]<sup>+</sup>.

**7.1.19. 3-Hydroxy-2-[[4-(4-methyl-1,4-diazepan-1-yl)benzoyl]amino]-*N*-(5-methyl-2-pyridyl)benzamide Hydrochloride (31)**

Compound **37**, which was prepared from 0.949 mmol of compound **10**, and compound **26** (210 mg, 0.864 mmol) were combined in pyridine (5 mL) and stirred at ambient temperature for 24 h. The reaction mixture was concentrated in vacuo. The residue was diluted with CHCl<sub>3</sub> and washed with 5% aqueous sodium bicarbonate. The organic layer was dried over magnesium sulfate and concentrated in vacuo. The residue was subjected to chromatography over silica gel eluting with CHCl<sub>3</sub>/MeOH (94:6 by volume). The resulting material was dissolved in 1 N hydrochloric acid and concentrated in vacuo. The residue was subjected to chromatography over ODS gel eluting with CH<sub>3</sub>CN/0.001 N hydrochloric acid (10:90 by volume) to give the title compound as a pale yellow amorphous powder (103 mg, 24%): <sup>1</sup>H NMR (400 MHz, DMSO-*d*<sub>6</sub>) δ 2.10–2.21 (1H, m), 2.28–2.40 (4H, m), 2.78 (3H, d, *J* = 4.9 Hz), 3.03–3.19 (2H, m), 3.38–3.54 (4H, m), 3.72–3.79 (1H, m), 3.83–3.94 (1H, m), 6.82 (2H, d, *J* = 9.3 Hz), 7.13–7.26 (3H, m), 7.84–7.91 (4H, m), 8.18 (1H, s), 9.78 (1H, s), 10.04 (1H, br s), 10.85 (1H, br s), 11.04 (1H, br s); FAB-MS *m/z* 459 [M+H]<sup>+</sup>; Anal. calcd for C<sub>26</sub>H<sub>29</sub>N<sub>5</sub>O<sub>3</sub>·1.7HCl·2H<sub>2</sub>O: C, 56.01; H, 6.27; N, 12.56; Cl, 10.81. Found: C, 55.86; H, 6.39; N, 12.73; Cl, 10.70.

**7.1.20. *N*-(5-Chloro-2-pyridyl)-3-hydroxy-2-[[4-(4-methyl-1,4-diazepan-1-yl)benzoyl]amino]benzamide Hydrochloride (32)**

The title compound was obtained from compound **27**<sup>19</sup> using the methods described for the synthesis of compound **19** as a colorless solid (37%): mp 229–231 °C; <sup>1</sup>H NMR (400 MHz, DMSO-*d*<sub>6</sub>) δ 2.17–2.26 (2H, m), 2.74 (3H, s), 3.00–3.60 (6H, m), 3.77–3.88 (2H, m), 6.82 (2H, d, *J* = 8.8 Hz), 7.10–7.25 (3H, m), 7.83 (2H, d, *J* = 8.8 Hz), 7.90 (1H, dd, *J* = 2.5 and 8.7 Hz), 8.13 (1H, d,

*J* = 8.7 Hz), 8.35 (1H, d, *J* = 2.5 Hz), 9.71 (1H, s), 9.95 (1H, s), 10.58 (1H, s), 10.75 (1H, br s); FAB-MS *m/z* 480 [M+H]<sup>+</sup>; Anal. calcd for C<sub>25</sub>H<sub>26</sub>N<sub>5</sub>O<sub>3</sub>Cl·HCl·0.7H<sub>2</sub>O: C, 56.76; H, 5.41; N, 13.24; Cl, 13.40. Found: C, 57.05; H, 5.18; N, 13.27; Cl, 13.02.

**7.1.21. 5-Chloro-*N*-(5-chloro-2-pyridyl)-3-hydroxy-2-[[4-(4-methyl-1,4-diazepan-1-yl)benzoyl]amino]benzamide Hydrochloride (33)**

Compound **37**, which was prepared from 3.00 mmol of compound **10**, and compound **28**<sup>19</sup> (891 mg, 2.99 mmol) were combined in pyridine (10 mL) and stirred at ambient temperature for 13 h. The reaction mixture was concentrated in vacuo. The residue was dissolved in acetic acid (20 mL) and the whole was stirred at ambient temperature for 17 h. The reaction mixture was concentrated in vacuo. The residue was diluted with CHCl<sub>3</sub> and washed with 5% aqueous sodium bicarbonate. The organic layer was dried over magnesium sulfate and concentrated in vacuo. The residue was subjected to chromatography over silica gel eluting with CHCl<sub>3</sub>/MeOH/c.NH<sub>3</sub> (100:5:0.5 by volume). The resulting material was dissolved in 1 N hydrochloric acid and concentrated in vacuo. The residue was subjected to chromatography over ODS gel eluting with CH<sub>3</sub>CN/0.002 N hydrochloric acid (3:7 by volume) to give the title compound as a colorless amorphous powder (492 mg, 31%): <sup>1</sup>H NMR (400 MHz, DMSO-*d*<sub>6</sub>) δ 2.10–2.21 (1H, m), 2.23–2.37 (1H, m), 2.79 (3H, d, *J* = 4.9 Hz), 3.02–3.21 (2H, m), 3.37–3.56 (4H, m), 3.66–3.95 (2H, m), 6.81 (2H, d, *J* = 8.8 Hz), 7.15 (2H, s), 7.82 (2H, d, *J* = 8.8 Hz), 7.89 (1H, dd, *J* = 2.4 and 8.8 Hz), 8.08 (1H, d, *J* = 8.8 Hz), 8.36 (1H, d, *J* = 2.4 Hz), 9.51 (1H, s), 10.49 (1H, br s), 10.68 (2H, br s); FAB-MS *m/z* 514 [M+H]<sup>+</sup>; Anal. calcd for C<sub>25</sub>H<sub>25</sub>N<sub>5</sub>O<sub>3</sub>Cl<sub>2</sub>·HCl·1.1H<sub>2</sub>O: C, 52.62; H, 4.98; N, 12.27; Cl, 18.64. Found: C, 52.48; H, 4.69; N, 12.23; Cl, 18.49.

**7.1.22. 5-Chloro-*N*-(5-chloro-2-pyridyl)-2-[[4-(4-methyl-1,4-diazepan-1-yl)benzoyl]amino]benzamide Hydrochloride (34)**

The title compound was obtained from 2-amino-5-chloro-*N*-(5-chloro-2-pyridyl)benzamide **29**<sup>25</sup> using the methods described for the synthesis of compound **19** as a colorless solid (87%): mp 254–257 °C; <sup>1</sup>H NMR (400 MHz, DMSO-*d*<sub>6</sub>) δ 2.12–2.20 (1H, m), 2.32–2.43 (1H, m), 2.78 (3H, d, *J* = 4.8 Hz), 3.05–3.20 (2H, m), 3.39–3.56 (4H, m), 3.73–3.82 (1H, m), 3.91–3.97 (1H, m), 6.90 (2H, d, *J* = 8.7 Hz), 7.65 (1H, dd, *J* = 2.4 and 8.8 Hz), 7.79 (2H, d, *J* = 8.7 Hz), 7.99–8.02 (2H, m), 8.11 (1H, d, *J* = 8.8 Hz), 8.43 (1H, d, *J* = 8.8 Hz), 8.48 (1H, d, *J* = 2.4 Hz), 10.94 (1H, br s), 11.23 (1H, s), 11.29 (1H, s); FAB-MS *m/z* 498 [M+H]<sup>+</sup>; Anal. calcd for C<sub>25</sub>H<sub>25</sub>N<sub>5</sub>O<sub>2</sub>Cl<sub>2</sub>·HCl·0.3H<sub>2</sub>O: C, 55.58; H, 4.96; N, 12.96; Cl, 19.69. Found: C, 55.68; H, 5.02; N, 12.73; Cl, 19.37.

**7.1.23. 3-[[4-(4-Methoxyphenyl)carbamoyl]-2-[[4-(4-methyl-1,4-diazepan-1-yl)benzoyl]amino]phenyl β-D-glucopyranosiduronic acid (35)**

Compound **11** (366 mg, 0.716 mmol) was suspended in CHCl<sub>3</sub> (50 mL) and washed with 5% aqueous sodium bicarbonate. The organic layer was dried over magnesium sulfate and concentrated in vacuo to yield a colorless powder. To a stirred mixture of the this material, methanol (3.5 mL), and CHCl<sub>3</sub> (3.5 mL) was added 1,8-diazabicyclo[5.4.0]undec-7-ene (436 mg, 2.86 mmol) at ambient temperature. After 30 min, to the reaction mixture was added acetobromo-α-D-glucuronic acid methyl ester (853 mg, 2.15 mmol) at ambient temperature, and the whole was stirred for 21 h. To the reaction mixture were added sodium carbonate (750 mg, 7.08 mmol) and H<sub>2</sub>O (4 mL) at ambient temperature, and the whole was stirred for 24 h. The reaction mixture was concentrated in vacuo. The residue was diluted with H<sub>2</sub>O, washed with CHCl<sub>3</sub>, and then extracted with *n*-butanol. The organic layer was concentrated in vacuo. The residue was diluted with H<sub>2</sub>O (5 mL), neutralized with acetic acid and concentrated in vacuo. The residue was



subjected to chromatography over ODS gel eluting with CH<sub>3</sub>CN/H<sub>2</sub>O (30:70 by volume) to give the title compound as a colorless amorphous powder (208 mg, 45%): <sup>1</sup>H NMR (400 MHz, DMSO-*d*<sub>6</sub>)  $\delta$  1.94–2.02 (2H, m), 2.44 (3H, s), 2.70–2.75 (2H, m), 2.84–2.90 (2H, m), 3.22–3.48 (6H, m), 3.62–3.65 (2H, m), 3.70 (3H, s), 3.78 (1H, d, *J* = 9.3 Hz), 4.95 (1H, d, *J* = 7.8 Hz), 5.17 (1H, br s), 5.39 (1H, br s), 6.75 (2H, d, *J* = 8.8 Hz), 6.84 (2H, d, *J* = 8.8 Hz), 7.29–7.34 (3H, m), 7.54 (2H, d, *J* = 8.8 Hz), 7.80 (2H, d, *J* = 8.8 Hz), 9.40 (1H, s), 10.04 (1H, s); FAB-MS *m/z* 651 [M+H]<sup>+</sup>; Anal. calcd for C<sub>33</sub>H<sub>38</sub>N<sub>4</sub>O<sub>10</sub>·3H<sub>2</sub>O: C, 56.24; H, 6.29; N, 7.95. Found: C, 56.36; H, 6.18; N, 7.96.

#### 7.1.24. 5-Chloro-3-[(5-chloro-2-pyridyl)carbamoyl]-2-[[4-(4-methyl-1,4-diazepan-1-yl)benzoyl]amino]phenyl β-D-glucopyranosiduronic acid (36)

The title compound was obtained from compound **33** using the methods described for the synthesis of compound **35** as a colorless amorphous powder (15%): <sup>1</sup>H NMR (400 MHz, DMSO-*d*<sub>6</sub>)  $\delta$  1.93–2.01 (2H, m), 2.45 (3H, s), 2.72–2.77 (2H, m), 2.87–2.91 (2H, m), 3.22–3.66 (8H, m), 3.84 (1H, d, *J* = 9.3 Hz), 5.06 (1H, d, *J* = 7.3 Hz), 5.21 (1H, br s), 5.49 (1H, br s), 6.73 (2H, d, *J* = 8.8 Hz), 7.37 (1H, d, *J* = 1.5 Hz), 7.43 (1H, d, *J* = 1.5 Hz), 7.77 (2H, d, *J* = 8.8 Hz), 7.87 (1H, dd, *J* = 2.4 and 8.8 Hz), 8.07 (1H, d, *J* = 8.8 Hz), 8.34 (1H, d, *J* = 2.4 Hz), 9.37 (1H, s), 10.81 (1H, br s); FAB-MS *m/z* 690 [M+H]<sup>+</sup>; Anal. calcd for C<sub>31</sub>H<sub>33</sub>N<sub>5</sub>O<sub>9</sub>Cl<sub>2</sub>·3H<sub>2</sub>O: C, 50.01; H, 5.28; N, 9.41; Cl, 9.52. Found: C, 50.27; H, 5.02; N, 9.55; Cl, 9.69.

## 7.2. Pharmacology

### 7.2.1. In vitro assay for inhibition of factor Xa

The hydrolysis rates of synthetic substrates were assayed by continuously measuring absorbance at 405 nm at 37 °C with a microplate reader (model 3550, Bio-Rad, U.S.). Reaction mixtures (125 μL) were prepared in 96-well plates containing chromogenic substrates (S-2222) and an inhibitor in either 0.05 M Tris-HCl, pH 8.4, or 0.15 M NaCl. Reactions were initiated with 25 μL of enzyme solution. The concentration of inhibitor required to inhibit enzyme activity by 50% (IC<sub>50</sub>) was calculated from dose–response curves in which the logit transformation of residual activity was plotted against the logarithm of inhibitor concentration.

### 7.2.2. Enzyme selectivity

Reaction mixtures were prepared in 96-well plates containing the chromogenic substrate and test compound. The reaction was initiated by the addition of enzyme, and the color was continuously monitored at 405 nm using a microplate reader SpectraMax 340PC (Molecular Devices, CA, U.S.) at 37 °C. Each enzyme was used at final concentration as follows: 0.20 U mL<sup>−1</sup> thrombin and 1.0 U mL<sup>−1</sup> trypsin. The enzymatic activities were assessed by the amidolysis of the following chromogenic substrates for the corresponding protease: S-2222 for trypsin and S-2238 for thrombin. The rate of substrate hydrolysis (mOD min<sup>−1</sup>) was measured at 37 °C. The mode of inhibition was estimated from a Lineweaver–Burk plot. The K<sub>i</sub> was determined from a Dixon plot by plotting the reciprocal of the initial reaction velocities at different substrate concentrations against different inhibitor concentrations.

### 7.2.3. Prothrombin time assays in vitro

After collection of citrated blood samples, platelet-poor plasma was prepared by centrifugation at 3000 rpm for 10 min and stored at −40 °C until use. Plasma clotting times were measured using a KC10A coagulometer (Amelung Co., Lehbrinsweg, Germany) at 37 °C. Prothrombin time (PT) was measured using Orthobrain thromboplastin (OrthoDiagnostic Systems Co., Tokyo, Japan), and values for each test sample were compared with coagulation times of a distilled water control. The concentration required to double

the clotting time (CT2) was estimated from each individual concentration–response curve. Each measurement was performed three times and represented as the mean value.

### 7.2.4. Ex vivo anticoagulant assays in mice

The test drug was dissolved or suspended in 0.5% methyl cellulose and orally administered to male ICR mice (mass range: 30–37 g) at a dose of 100 mg/kg using a gastric tube. Citrated blood was collected from the inferior vena cava 0.5 and 2.0 h after oral administration, and platelet-poor plasma was prepared by centrifugation for measurement of PT. All data were expressed as relative-fold values, compared with the baseline value of vehicle-treated mice.

## 7.3. Computational simulations

### 7.3.1. Preparation of fragment matrix

Common substructures were extracted in the set of 26 compounds, and R-group decomposition was executed for the common substructure as a query. A collection of 26 combinations of scaffolds and fragments were tabled as all of them were allocated in one matrix, in which rows corresponded to scaffolds and columns to substituents. Rows and columns were ordered by hierarchical clustering (average linkage) by Tanimoto distance with RDKit<sup>38</sup> morgan fingerprint (1024 bits, radius = 2) in KNIME workflow<sup>39</sup>, respectively. The dendrogram of clustering for the scaffolds was depicted on the right outer side, and that for fragments was on the upper side. Scaffold and fragment was expressed with the smiles notation on the left outer side and the lower side, respectively. Each cell was colored with red as low potency via yellow to green as high potency.

### 7.3.2. Estimation with slope one algorithm

Measured values of oral PT–prolongation effect in fragment matrix were transformed into PT indexes with following equation: PT index = log<sub>10</sub>(PT/controlPT-1). Imputation for missing data in the matrix was executed with Slope One algorithm<sup>36</sup> and following inverse transformation to afford estimated values of PT–prolongation effect for nonsynthesized compounds.

## Acknowledgments

The authors deeply acknowledge Drs. Shuichi Sakamoto, Tomihisa Kawasaki, and Takeshi Shigenaga for useful discussion. The authors also thank to Dr. Takeshi Kadokura for pharmacokinetic analysis. The authors are grateful to Ms. Yumiko Moritani for performing pharmacological experiments. The authors would like to express our gratitude to Mr. Norio Seki for solution-phase synthesis of library compounds and the staff of the Division of Analytical & Pharmacokinetics Research Laboratories for the elemental analysis and spectral measurements.

## References and notes

- Hirsh, J. N. *Engl. J. Med.* **1865**, 1991, 324.
- Stein, P. D.; Grandison, D.; Hua, T.; Slettehaugh, P. M.; Henry, J. W.; Turlapaty, P.; Kerwin, R. *Postgrad. Med. J.* **1994**, 70, S72.
- Hirsh, J.; Poller, L. *Arch. Int. Med.* **1994**, 154, 282.
- Bona, R. D.; Hickey, A. D.; Wallace, D. M. *Thromb. Haemost.* **1997**, 78, 137.
- Kaiser, B. *Cell. Mol. Life Sci.* **2002**, 59, 189.
- Samama, M. M. *Thromb. Res.* **2002**, 106, V267.
- Walenga, J. M.; Jeske, W. P.; Hoppensteadt, D.; Fareed, J. *Curr. Opin. Invest. Drugs* **2003**, 4, 272.
- Sitko, G. R.; Ramjit, D. R.; Stabilito, I. I.; Lehman, D.; Lynch, J. J.; Vlasuk, G. P. *Circulation* **1992**, 85, 805.
- Lynch, J. J.; Sitko, G. R.; Lehman, E. D.; Vlasuk, G. P. *Thromb. Haemost.* **1995**, 74, 640.
- Pinto, D. J. P.; Smallheer, J. M.; Cheney, D. L.; Knabb, R. M.; Wexler, R. R. *J. Med. Chem.* **2010**, 53, 6243, and references cited therein.
- Nagahara, T.; Yokoyama, Y.; Inamura, K.; Katokura, S.; Komoriya, S.; Yamaguchi, H.; Hara, T.; Iwamoto, M. *J. Med. Chem.* **1994**, 37, 1200.

12. Roehrig, S.; Straub, A.; Pohlmann, J.; Lampe, T.; Pernerstorfer, J.; Schlemmer, K. H.; Reinemer, P.; Perzborn, E. *J. Med. Chem.* **2005**, *48*, 5900.
13. Pinto, D. J. P.; Orwat, M. J.; Koch, S.; Rossi, K. A.; Alexander, R. S.; Smallwood, A.; Wong, P. C.; Rendina, A. R.; Luettgen, J. M.; Knabb, R. M.; He, K.; Xin, B.; Wexler, R. R.; Lam, P. Y. S. *J. Med. Chem.* **2005**, *50*, 5339.
14. Chung, N.; Jeon, H. K.; Lien, L. M.; Lai, W. T.; Tse, H. F.; Chung, W. S.; Lee, T. H.; Chen, S. A. *Thromb. Haemost.* **2011**, *105*, 535.
15. Masters, J. J.; Franciskovich, J. B.; Tinsley, J. M.; Campbell, C.; Campbell, J. B.; Craft, T. J.; Froelich, L. L.; Gifford-Moore, D. S.; Hay, L. A.; Herron, D. K.; Klimkowski, V. J.; Kurz, K. D.; Metz, J. T.; Ratz, A. M.; Shuman, R. T.; Smith, G. F.; Smith, T.; Towner, R. D.; Wiley, M. R.; Wilson, A.; Yee, Y. K. *J. Med. Chem.* **2000**, *43*, 2087.
16. Pinto, D. J. P.; Orwat, M. J.; Wang, S.; Fevig, J. M.; Quan, M. L.; Amparo, E.; Cacciola, J.; Rossi, K. A.; Alexander, R. S.; Smallwood, A. M.; Luettgen, J. M.; Liang, L.; Aungst, B. J.; Wright, M. R.; Knabb, R. M.; Wong, P. C.; Wexler, R. R.; Lam, P. Y. S. *J. Med. Chem.* **2001**, *44*, 566.
17. Hirayama, F.; Koshio, H.; Katayama, N.; Kurihara, H.; Taniuchi, Y.; Sato, K.; Hisamichi, N.; Sakai-Moritani, Y.; Kawasaki, T.; Matsumoto, Y.; Yanagisawa, I. *Bioorg. Med. Chem.* **2002**, *10*, 1509.
18. Hirayama, F.; Koshio, H.; Ishihara, T.; Hachiya, S.; Sugawara, K.; Koga, Y.; Seki, N.; Shiraki, R.; Shigenaga, T.; Iwatsuki, Y.; Moritani, Y.; Mori, K.; Kadokura, T.; Kawasaki, T.; Matsumoto, Y.; Sakamoto, S.; Tsukamoto, S. *J. Med. Chem.* **2011**, *54*, 8051.
19. Ishihara, T.; Koga, Y.; Sugawara, K.; Mori, K.; Iwatsuki, Y.; Hirayama, F. Accepted in *Bioorg. Med. Chem.*
20. Free, S. M.; Wilson, J. W. *J. Med. Chem.* **1964**, *7*, 395.
21. Kubinyi, H. *Quant. Struct.-Act. Relat.* **1988**, *7*, 121.
22. Koshio, H.; Hirayama, F.; Ishihara, T.; Shiraki, R.; Shigenaga, T.; Taniuchi, Y.; Sato, K.; Moritani, Y.; Iwatsuki, Y.; Kaku, S.; Katayama, N.; Kawasaki, T.; Matsumoto, Y.; Sakamoto, S.; Tsukamoto, S. *Bioorg. Med. Chem.* **2005**, *13*, 1305.
23. Reisch, J.; Gunaherath, G. M. K. B. *Monatsh. Chem.* **1988**, *119*, 1169.
24. Yoshino, H.; Tsuchiya, Y.; Saito, I.; Tsujii, M. *Chem. Pharm. Bull.* **1987**, *35*, 3438.
25. Beight, D. W.; Craft, T. J.; Denny, C. P.; Franciskovich, J. B.; Goodson, T. Jr.; Hall, S. E.; Herron, D. K.; Joseph, S. P.; Klimlowski, V. J.; Masters, J. J.; Mendel, D.; Milot, G.; Pineiro-Nunez, M. M.; Sawyer, J. S.; Shuman, R. T.; Smith, G. F.; Tebbe, A. L.; Tinsley, J. M.; Weir, L. C.; Wikel, J. H.; Wiley, M. R.; Yee, Y. K. (Eli Lilly and Co, USA). PCT Int. Appl. WO2000039118, 2000; *Chem. Abstr.* **2000**, *133*, 89437h.
26. Berrang, B.; Brine, G. A.; Carrol, F. I. *Synthesis* **1997**, 1165.
27. Schmidt, R. R.; Grundler, G. *Synthesis* **1981**, 886.
28. Badman, G. T.; Green, D. V. S.; Voyle, M. J. *Organomet. Chem.* **1990**, *388*, 117.
29. Holloway, C. J.; Zierhut, M. *IRCS Med. Sci.: Library Compendium* **1981**, *9*, 96.
30. Ebner, T.; Burchell, B. *Drug Metab. Dispos.* **1993**, *21*, 50.
31. Shimizu, M.; Matsumoto, Y.; Tatsuno, M.; Fukuoka, M. *Biol. Pharm. Bull.* **2003**, *26*, 216.
32. Adler, M.; Kochanny, M. J.; Ye, B.; Rumennik, G.; Light, D. R.; Biancalana, S.; Whitlow, M. *Biochemistry* **2002**, *41*, 15514.
33. Francesco Ricci, F.; Rokach, L.; Shapira, B., *Introduction to Recommender Systems Handbook*, Springer, **2011**, pp. 1–35 and references cited therein.
34. Wassermann, A. M.; Haebel, P.; Weskamp, N.; Bajorath, J. *J. Chem. Inf. Model.* **2012**, *52*, 1769.
35. Gupta-Ostermann, D.; Shanmugasundaram, V.; Bajorath, J. *J. Chem. Inf. Model.* **2014**, *54*, 801.
36. Lemire, D., Maclachlan, A. SIAM Data Mining (SDM'05), Newport Beach, California, April 21–23, 2005.
37. Coyne, W. E.; Cusic, J. W. *J. Med. Chem.* **1968**, *11*, 1208.
38. RDKit: Open-Source Cheminformatics. <http://www.rdkit.org>.
39. KNIME: The Konstanz Information Miner. <http://www.knime.org>.